POLITECNICO
MILANO 1863

SCUOLA DI INGEGNERIA INDUSTRIALE
E DELL'INFORMAZIONE

Executive Summary of the Thesis

Study of optimized HTS solenoid configurations for the beam cooling of a Muon Collider

Laurea Magistrale in Nuclear Engineering - Ingegneria Nucleare

Author: Jonathan Pavan

Advisor: Prof. Marco Beghi

Co-advisors: Prof. Lucio Rossi: UNIMI, Prof. Marco Statera: INFN-LASA (Milan)
Dr. Luca Bottura, Dr. Bernardo Bordini: CERN, Geneva (Switzerland)

Academic year: 2022-2023

1. Motivations

In 1911, the Dutch physicist Heike Kamerlingh Onnes discovered superconductivity, a phenomenon for which certain materials can conduct electric current without resistance when cooled to very low temperatures. Superconductivity has since become a technology that has contributed to advancements in various fields such as medicine, transportation, electronics, and astronomy. The remarkable ability of superconductors to carry large electric currents without resistance has been also harnessed in the design of magnets for high-energy physics, particularly in particle accelerators. Scientists aim to develop magnets with increasingly higher magnetic fields to accelerate particle bunches faster and faster and more and more tightly, to delve into the mysteries of the Universe. The Muon Collider is one the options being considered for the next generation of particle accelerators. Unlike other machines, the Muon Collider will accelerate muons, which are particles similar to electrons but 200 times heavier and decay within a very short time. This thesis focuses on the solenoids of the 6D Cooling stage of the Muon Collider, which pose technical and design barriers, due to the inherent nature of muons.

2. Introduction

2.1. History

The story of the discovery of superconductivity is inexorably linked to the technological advances in the field of cryogenics, but also to the scientific progress of the concept of electrical resistivity. Driven by the achievement of increasingly cold temperatures, Cailletet and other researchers conducted studies on the conductivity of metals, finding a proportional increase in conductivity as temperature decreased. This led to investigations on the behavior of resistivity near absolute zero, with three different predictions emerging. Dewar hypothesized that at 0 K, resistivity would be zero. Kelvin proposed a minimum point of resistivity, while Matthiessen's model suggested the existence of a plateau in resistivity at low temperatures, influenced by impurity levels. Kamerlingh Onnes attempted to reduce impurities in a specimen to test if resistivity would drop to zero, choosing mercury due to the ease of distilling it to high purity levels. Using a mercury resistor, he observed

a remarkable drop in resistivity to "practically zero" at temperatures below 4.2 K, leading to the groundbreaking discovery of superconductivity.
In 1986, Bednorz and Müller discovered a copper-based ceramic material that exhibited superconductivity at a relatively high temperature of 35 K (−238.15 °C). Another significant contribution to the field of high-temperature superconductivity was made by Paul Chu and his team in 1987. They achieved superconductivity at even higher temperatures using a ceramic material composed of yttrium, barium, copper, and oxygen, which exhibited superconductivity at 93 K. High Temperature Superconductors, from this time forward, gained significant prominence and widespread use.

2.2. Theory

The thesis explores the initial phenomenological theories of the two-fluid model and the London theory, delves into the thermodynamic aspects of superconductors, and analyzes the quantum mechanical theories of Ginzburg-Landau and the BCS theory, which have significantly contributed to our understanding of superconductivity. Due to the extensive range of theoretical aspects covered in this thesis, it is impractical to summarize all of them concisely in just a few lines. Conversely, it is noteworthy to provide a brief overview of the subsequent paragraph which explores the intriguing aspects of HTS and the difference between Type I and Type II superconductors. Type I superconductors never allow the magnetic field to penetrate inside them. They have just one critical magnetic field B_c and if $B < B_c$ and $T < T_c$ they are said to be in the Meissner state: they superconduct, show perfect diamagnetism and their magnetization M is everywhere (a part for the London penetration depth) equal and opposite in direction with respect to the magnetic field H. From an engineering point of view, they are not useful because their $B_c = \mu_0 H_c$ are extremely low (less than 0.1 T) and then they can sustain only small current densities. Type II superconductors have two critical magnetic fields, $B_{c1} = \mu_0 H_{c1}$ and $B_{c2} = \mu_0 H_{c2}$, respectively the lower and the upper critical field. Both B_{c1} and B_{c2} are temperature dependant and in order for the metal to superconduct, of course, it has to be maintained, as usual, to a temperature below its critical temperature T_c. In the range $0 < B < B_{c1}$ the superconductor is said to be in the *Meissner* state. Here its behaviour is very similar to that of a Type I. Instead, in the range $B_{c1} < B < B_{c2}$ it is in the so–called *mixed* state because inside the material one can find both a normal and a superconducting phase. Type II superconductors are usually able to carry a considerably higher amount of current than any other material.
Among the category of Type II superconductors, there is a special set of materials called *high temperature* superconductors, HTS for short. They have the outstanding ability to superconduct above the liquid nitrogen temperature (77 K). This property will be important in future applications because liquid nitrogen is extremely less expensive than liquid helium. The main class of high–T_c is the cuprate superconductors. They are sometimes called ReBCO to highlight their composition: one Rare–earth and barium compound and a copper oxide layer.

3. Muon Collider

Exploring a Muon Collider instead of another proton collider presents several compelling reasons that make it an intriguing avenue to broaden our horizons [4]. Among them, one of the most important is depicted in Figure 1.

Figure 1: Equivalent proton collider energy

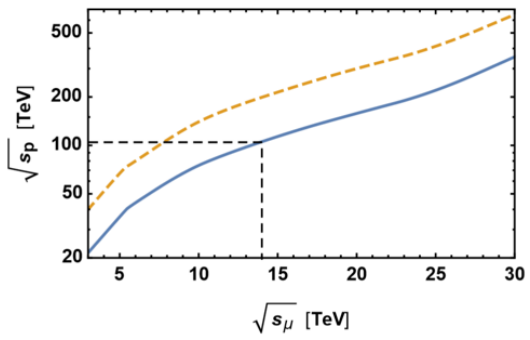

The plot shows the center of mass energy $\sqrt{s_p}$ that a proton collider should have to be "equivalent" to a muon collider of $\sqrt{s_\mu}$. A 14 TeV muon collider has the potential to provide a similar discovery reach as a 100 TeV proton collider. A comparison among different machines shows that the Muon Collider's efficiency increases

with energy. At energy levels above approximately 3 TeV, the Muon Collider is expected to be the most energy-efficient choice. The Muon Collider offers great physics potential as a Higgs factory, benefiting from the higher s-channel coupling of muons compared to electrons and the substantial Higgs production cross section. Additionally, the use of muons, which have a larger mass, significantly lowers synchrotron radiation losses. A muon collider can naturally achieve both high-energy collisions and high luminosity measurements. The design of such a collider is distinct due to the unique characteristics of muons: their production through nuclear reactions and their inherent instability, decaying within 2.2 μs.

The US Muon Accelerator Program (MAP, 2011-2014) can be considered as one of the first step in the direction of obtaining a real concept of a muon collider. The design at which it arrived can be seen from Figure 2. The Muon Collider consists of five different stages: the proton driver, the front end, the cooling, the acceleration and finally the collider ring.

Given that the objectives of the thesis work are the superconductive solenoids of the cooling stage, it is worthwhile to provide a more detailed description of it. When muons enter the cooling stage they occupy a large volume in phase-space, which then has to be reduced by several orders of magnitude. Considering the muon lifetime, the only viable method is the *6D ionization cooling*. By means of ionization energy loss in absorbers the beam momentum is reduced in every directions but it is then only replenished in the longitudinal one through RF cavities (transverse cooling). The dispersive beam is let pass through properly designed wedge-shaped absorbers such that the low-energy particles traverse less material and are longitudinally cooled less, and vice versa. The net result is a reduction of the longitudinal emittance at the expense of the transverse one. The emittance is then exchanged in the two directions and can be later "removed" by the ionization cooling. This emittance exchange, together with the ionization, accounts for the complete 6D cooling of the muon bunches. The 6D ionization cooling consists of a lattice of 12 different unique stage types, where each stage is a repeating series of a cell type. The number of cells in a stage ranges from 20 to 130, and the total length over 12 stages is 0.9 km. There are four stages before bunch recombination and 8 stages after bunch recombination. In each cell there are from a minimum of two solenoids up to a maximum of six and magnets on the left have opposite polarity with respect to those on the right (configuration which generates a sinusoidally varying magnetic field on-axis). Each cell is composed also of RF cavities and absorbers.

4. Solenoids

One of the goals of this thesis work has been the initial characterization of the 2954 solenoids which are used in the *6D Cooling* stage of the Muon Collider. It should be emphasized that the magnets described in the US MAP study were primarily designed to fulfill the beam dynamics requirement of producing the appropriate magnetic field on-axis. However, the majority of these magnets were not subjected to a comprehensive engineering analysis to assess their feasibility. The first step in this direction has been the initial characterization of the magnetic and mechanical properties of the 18 unique solenoids that constitute the 12 different stages of the Cooling. To achieve this goal, various tools were employed. Specifically, I developed

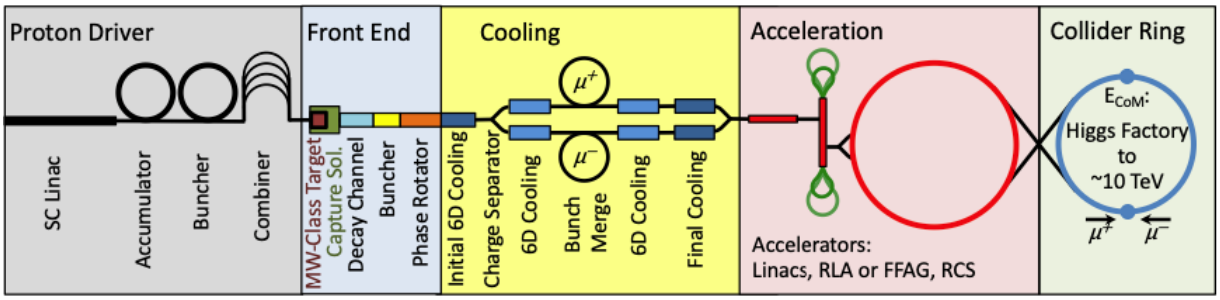

Figure 2: The US MAP design of the Muon Collider, from [3]

MATLAB codes to evaluate analytical formulas, and I set up Finite Element Models (FEMs) using Comsol Multiphysics.

4.1. Magnetic and Mechanical Analysis

A *solenoid*, within the area of accelerator magnets, is an electromagnet usually characterized by a rectangular section of a wound coil of wire. The simplest configuration involves just a rectangular cross-section. The magnetic field produced by a general distribution of current can be evaluated from integration of the Biot-Savart law

$$\boldsymbol{B}(\boldsymbol{r}) = \frac{\mu_0}{4\pi} \int_V \frac{\boldsymbol{J}(\boldsymbol{r}') \times (\boldsymbol{r} - \boldsymbol{r}')}{|\boldsymbol{r}' - \boldsymbol{r}|^3} \, d^3r'. \qquad (1)$$

To evaluate the magnetic field of a finite real solenoid there are several methods which have been used in literature (mainly elliptical integrals). The method [2] used makes use of infinite series of partial binomial expansions. This approach turned out to be particularly simple to be implemented in a numerical code and precise enough in those regions of special interest, like the on-axis field and the bore volume closest to the axis. Several analytical formulas have been used to evaluate quantities like the self-inductances, the mutual inductances, the magnetic stored energy.
Another important aspect to be taken into account when designing a magnet is the mechanical stress-strain analysis. The magnetic field exerts a so-called Lorentz force per unit volume on the current-carrying conductor [5]

$$\boldsymbol{F}_L = \boldsymbol{B} \times \boldsymbol{J}. \qquad (2)$$

Because of Eq (2), the force exerted by the interaction between the magnetic field and the current flowing inside the conductor tends to push the solenoid outward radially. The solenoid behaves similarly to a cylinder under internal pressure. The solution of the elastic problem for a solenoid requires to take Eq (2) as the body force density, the equilibrium, constitutive, and compatibility equations and the proper boundary conditions. These mechanical calculations necessitate computer programs and the software that has been used was Comsol Multiphysics.

4.2. Results

The objective of this work was to characterize each stage and solenoid in terms of their magnetic and mechanical properties. Each stage has been studied in two different configurations: the first one considers just a single cell as standalone ("single cell"), while the other, which is more realistic, considers the cell as part of an infinite lattice of identical cells ("periodic"). The periodic simulation is representative of the inner cells of a real periodic lattice. Indeed, the fact that the real lattice is not infinite but has a starting and ending point spoils the perfect periodic symmetry.

Figure 3: Cell A1 on-axis B_z.

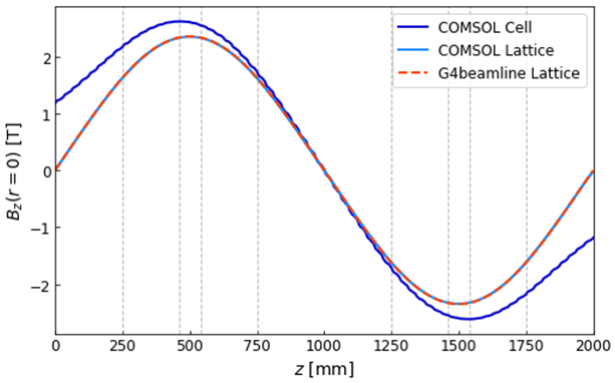

Fig 3 shows the magnetic field on-axis of Cell A1 (which has been taken as a case study) for the two configurations: the periodic symmetry imposes the field no be zero at the extremities. Furthermore, its magnitude appears smaller throughout the cell length.

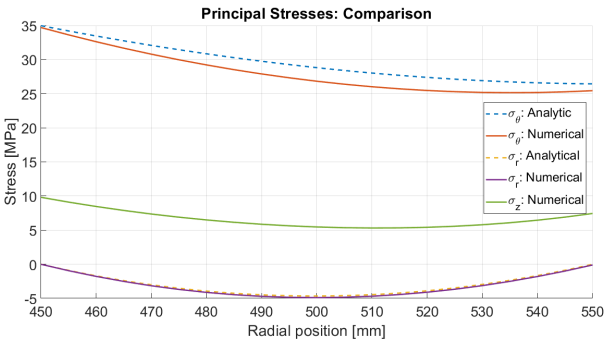

Figure 4: Cell A1 stress state.

Fig 4 shows a comparison between the analytical formulas and the numerical result in Comsol of the stress state. The next step has been

to evaluate magnetic properties like the maximum field on the conductor (essential parameter for a magnet designer), the self and mutual inductances of the solenoids within a cell, the magnetic stored energy and the stray fields, and mechanical quantities like the axial, hoop and radial stresses (and hence the maximum values) and the longitudinal axial net force between adjacent magnets, for all the 18 different cell types.

5. Quench

5.1. The phenomenon

The *quench* is Achilles' heel of superconductivity and, in particular, of superconducting magnets. Chapter 5 first explains what a quench is from a phenomenological point of view, introducing analytical formulas where possible, and then presents the finite element method (FEM) simulation I created and the corresponding results. While this is only a preliminary approach, it can still offer valuable insights in the field. A quench is a transition from a superconducting to a normal resistive state [1]. This transition, within a superconducting cable, cannot go unnoticed, as both the current density and the resistance in the normal state are large. The superconductor goes from being an exceptional conductor which carries electricity with virtually zero resistance to a state comparable to that of an insulator. The copper layer (the stabilizer), which is used to take momentarily care of the current during the quench, produces an extraordinary amount of Joule heating, causing the hot-spot (localized quench point) to reach, within seconds, temperatures that can exceed, if no protection mechanism is activated, hundreds of kelvins. In this process the stored magnetic energy of the magnet can be totally converted into heat. The quench phenomenon is quite complex as it is inherently a multiphysics event. Indeed, the quench also leads to the appearance of a voltage in the magnet and in particular across the quenched region, and to a differential thermal expansion that, together with the electro-magnetic forces, induces a stress state inside the conductor (and many other aspects like the evolution of the cooling helium). The phenomenon can hence be described by employing a complex system of coupled partial and total differential equations, among which, the most representative is the heat balance equation

$$C_i(T_i)\frac{\partial T_i}{\partial t} = \nabla \cdot [k_i(T_i)\nabla T_i] + \boldsymbol{J}_i \cdot \boldsymbol{E}_i + g_{d,i}(t) - g_{c,i}(t,T), \quad (3)$$

where $\boldsymbol{J}_i \cdot \boldsymbol{E}_i$ is the Joule heating ($= \rho_i J^2$), $g_{d,i}(t)$ represents any possible cause of quench initiation and $g_{c,i}(t,T)$ is the cooling term. Together with equations describing the evolution of currents (and voltages) in the electrical circuits, the state equation of helium, and possibly others such as an elastic problem, they collectively constitute a comprehensive description of the quench phenomenon. However, an analytical solution for the quench phenomenon does not exist, necessitating the use of simplified approaches. In the thesis, the concepts of hot-spot, minimum propagating zone (MPZ), minimum quench energy (MQE) safety margin and quench velocity are discussed and analyzed.

5.2. The Comsol Simulation

This introduction emphasizes the challenge of studying quenches and highlights the reliance on numerical simulations to comprehensively and reliably understand their dynamics and the behavior of quenched magnets. For this purpose, I implemented a 1D FEM simulation of a quench event in an HTS cable using Comsol Multiphysics. A 20 m long cable is the fundamental component of the simulation. It is initially at T_{op}, which is also the temperature at which the two extremities are fixed to (BC). The tape is composed of copper, hastelloy and YBCO but its properties (thermal and electrical conductivities, specific heat, and density) are the results of an homogenization with respect to the volumetric ratios of the different materials. Almost all materials properties are temperature dependant (making the problem highly non-linear) but copper (th. and el.) conductivities are also magnetic field and RRR (Residual-resistivity ratio $RRR = \rho_{T_{amb}}/\rho_{0\mathrm{K}}$) dependant and YBCO el. conductivity is expressed by means of its power law. An engineering current density of J_{op} is injected and once the system has reached equilibrium a Gaussian power density impulse is applied on a central region of length L_q. This disturbance, depending on its characteristics, can or cannot initiate a quench. If the quench is initiated, the model is able to study two different

aspects. In the first, the magnet (which in my approximation is represented by the 1D cable) is connected to a safety circuit (a RL circuit) which allows the huge magnetic energy to dissipate on a dump resistor. In this case a important output parameter is the maximum temperature reached by the system at the end of the quench event. This is an important tool from a quench protection point of view.

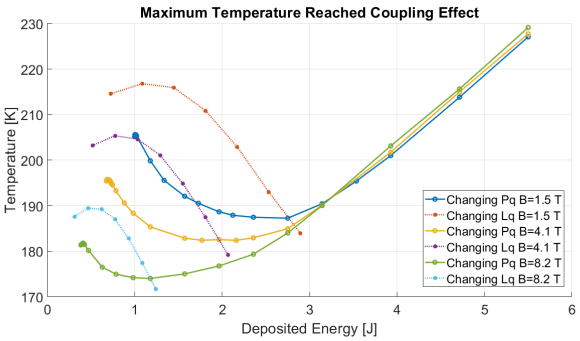

Figure 5: T_{max} at different B.

Fig 5 shows the maximum temperature reached (solid lines) at different peak values of the Gaussian disturbance and at three different values of background magnetic field. The plot shows that it is more complicated to protect a magnet at lower fields. Similar plots have been obtained changing copper RRR and the operational temperature, and evaluating the effects on the final temperature.
The second aspect is related to the quench velocity. The safety circuit is deactivated, the passage of the normal-superconducting wavefront is detected in 8 detection points and the velocity is deduced. Also here, the effects of the variation of some chosen parameters on the propagation velocity are evaluated. In particular, it has been found that the peak value of the Gaussian and the length of the domain on which it is applied do not influence the stationary propagation velocity, as expected. Furthermore, a modest increase in velocity has been observed with increasing magnetic field and operational temperature. Conversely, a decrease with respect to copper RRR was shown. Additionally, a linear dependence of the velocity on the current density has been identified. It is important to note the main characteristic of HTS cables is that, irrespective of the specific set of applied conditions the quench propagation velocities (few cm/s) are orders of magnitude smaller than those of LTS (several m/s).

6. Conclusions

This work has investigated the 6D Cooling stages of the Muon Collider and their solenoids. The analysis was based on input parameters from the US MAP study and encompassed two main aspects: the magnetic and mechanical considerations on one side, and the quench protection analysis on the other. In the initial paragraphs of Chapter 4, the description of the analytical formulas, the FEM model in Comsol Multiphysics, and the methodology employed are provided. Finally, a comprehensive overview of the results is presented. The analysis sheds light not only on the characteristics of the 18 different types of solenoids involved but also, and perhaps more importantly, on their weak points. It becomes evident that certain magnet parameters need to be optimized from an energy, cost, and engineering perspective. The solenoids are found to have high values of self-inductance and stored magnetic energy. Cell B1 alone, for example, has a stored energy of 44.5 MJ. As a reference, an LHC dipole, which is 15 m long and generates a field greater than 8 T, stores approximately 7 MJ of energy. It is crucial to emphasize the significance of these two parameters, particularly in the context of quench protection. Still considering the magnetic aspect, it is interesting to observe the difference between the peak value of the field on the axis compared to the value reached on the conductor. Depending on the stage and the solenoid, this ratio can be as high as approximately 3. Moreover, the mechanical analysis has also brought to light certain points of concern. Several solenoids experience hoop stress values exceeding 150 MPa, which can be considered a threshold value indicating the necessity for a mechanical support structure. If the presence of the structure was already assumed to be necessary, the evaluated longitudinal force values (as high as 3700 tons), on the other hand, highlight the fact that this structure must be highly complex. The last aspect is related to the tensile radial stress state which some magnets experience. It has been emphasized that this condition is unfavorable for solenoids, and several possible solutions were presented to address this issue.
Chapter 5 provides an introductory yet compre-

hensive analysis of the quench protection aspects. Despite the presence of existing software that model the quench phenomenon, a deliberate decision was made to develop a dedicated tool that, while not entirely general, offers complete control by allowing the selection of desired parameters from a vast configuration space. This choice allows for the analysis of the fundamental aspects of the phenomenon and serves as a solid foundation for future developments. The results presented in this chapter should be interpreted in light of the reasoning described above. These results are related to two distinct yet equally important considerations. The first aspect primarily focuses on the maximum temperature attained inside the cable, which is a significant concern during magnet quench events. The second involves the evaluation of the quench propagation velocity, which is vital for understanding the dynamics of the quench process itself. Lastly, it is worth highlighting the implementation of an application based on the existing simulation model. The aim of this application is to share and to provide a tool that can be accessed and utilized by anyone, even without the need for an expensive Comsol license.

This thesis work has been done in collaboration with

UNIVERSITÀ
DEGLI STUDI
DI MILANO

References

[1] Yukikazu Iwasa. *Case Studies in Superconducting Magnets: Design and Operational Issues*. Selected Topics in Superconductivity. Springer New York, 2 edition, 2009.

[2] Qiong-Gui Lin. An approach to the magnetic field of a finite solenoid with a circular cross-section. *European Journal of Physics*, 42(3):035206, March 2021.

[3] Mark Palmer. The us muon accelerator program. *arXiv preprint arXiv:1502.03454*, 2015.

[4] Daniel Schulte and Mark et al. Palmer. Bright muon beams and muon colliders. In Nicolas Mounet, editor, *European Strategy for Particle Physics - Accelerator R&D Roadmap*, number CERN-2022-001, page 145. CERN Yellow Reports: Monographs, 2022.

[5] M.N. Wilson. *Superconducting Magnets*. Monographs on cryogenics. Clarendon Press, 1983.